Exponential dependence of the vortex pinning potential on current density in high-T_c superconductors

H. Yan,* M. M. Abdelhadi,† and J. A. Jung‡
Department of Physics, University of Alberta, Edmonton, Alberta, T6G 2J1, Canada

B. A. Willemsen and K. E. Kihlstrom
Superconductor Technologies, Santa Barbara, California 93111-2310, USA
(Received 9 March 2004; revised manuscript received 7 October 2004; published 25 August 2005)

We investigated the dependence of the vortex pinning potential on current density $U_{eff}(J)$ in $Tl_2Ba_2CaCu_2O_y$, $Tl_2Ba_2Ca_2Cu_3O_y$, and $YBa_2Cu_3O_y$ thin films and single crystals, measured by us and other research groups. In all these cases $U_{eff}(J)$ was calculated from the magnetic relaxation data using Maley's procedure [Phys. Rev. B **42**, 2639 (1990)]. We explored the exponential dependence of $U_{eff}(J)$, first introduced by Thompson *et al.* [Phys. Rev. B **44**, 456 (1991).] to explain long-term nonlogarithmic magnetic relaxations in high-temperature superconductors (HTSC), as an alternative to power-law and logarithmic forms of $U_{eff}(J)$. The results revealed that for J larger than approximately $0.4J_c$, the energy barrier can be expressed in the following form: $U_{eff}(J)=aI_{co}(1-T/T^*)^{3/2}\exp(-bJ/J_{co})$, where the constant b is the same for all samples investigated. This result is independent of the anisotropy (the interplanar coupling). The experimental results were analyzed taking into account the spatial dependence of the pinning potential, proposed by Qin *et al.* [J. Appl. Phys. **77**, 2618 (1995)]. We suggested that the exponential form of $U_{eff}(J)$ could represent vortex pinning and motion in the *a-b* planes due to a nanoscopic variation of the order parameter, in agreement with the growing experimental evidence for the presence of nanostructures, stripes (filaments) in HTSC.

DOI: 10.1103/PhysRevB.72.064522 PACS number(s): 74.25.Qt, 74.25.Sv, 74.78.Na, 74.81.−g

I. INTRODUCTION

Because high-temperature superconductors (HTSC) are characterized by a very short Ginzburg-Landau coherence length, suppression of the superconducting order parameter can occur locally at a single atomic site due to deviations from stoichiometry caused, for example, by the presence of an oxygen vacancy or an impurity atom. Oxygen vacancies provide randomly distributed weak pinning centers. The effect of pinning of flux-line lattice by this type of randomly distributed weak point defects was considered by the collective pinning model of Larkin and Ovchinnikov.[1] Weak local pinning could be also produced by an intrinsic array of Josephson junctions. Studies of $YBa_2Cu_3O_y$ [YBCO(123)] crystals with a high-resolution transmission electron microscopy (HRTEM) by Etheridge[2] followed by more recent studies of $Bi_2Sr_2CaCu_2O_y$ [BSCCO(2212)] crystals with a sensitive scanning tunneling spectroscopy (STM) by Pan *et al.*[3] revealed the presence of a network of cells of size approximately 2–3 nm in the CuO_2 planes of these compounds. According to Etheridge, these cells have a ferroelastic origin, i.e., they are formed in the CuO_2 planes in a struggle to relieve internal stresses. Related STM work by Lang *et al.*[4] on BSCCO(2212) crystals suggested that the cells (the nanograins) could be coupled by Josephson tunnel (proximity) junctions forming a Josephson junction array in the *a-b* planes. Bearing this in mind, such an array could act as a source of periodically distributed weak pinning sites.

Extended crystal growth defects such as twin boundaries, grain boundaries, stacking faults, screw dislocations, and antiphase boundaries are expected to provide strong pinning sites for vortices in HTSC. Extended defects in *c*-axis-oriented epitaxial thin films of YBCO, like screw dislocations and antiphase boundaries along the *c* axis, are easily introduced during thin film growth on a single crystal substrate because of the crystal lattice mismatch between the substrate and the film, and also because of the surface roughness of the substrate.[5–8] Therefore one should not expect the presence of a large density of such defects in bulk YBCO single crystals, for example. Screw dislocations along the *c* axis are also less likely to be formed in BSCCO(2212) or $Tl_2Ba_2CaCu_2O_y$ [TBCCO(2212)] compounds.[9] This is because the large *c*-axis anisotropy of these materials results in the layer-by-layer growth of CuO_2 weakly coupled planes that occurs with a much faster rate in the *a* and *b* directions than along the *c* axis. Twin boundaries are absent in tetragonal compounds of BSCCO and TBCCO, however, they are present in orthorhombic YBCO(123), where they act as very efficient pinning centers.[10]

Therefore, one could anticipate that measurements of magnetic relaxation (i.e., a time decay of magnetization) in epitaxial thin films or in single crystals of YBCO, as a function of temperature, applied magnetic field, or applied transport current, would produce results dramatically different from those obtained on TBCCO (BSCCO) thin films or crystals, for example. Magnetic properties of optimally doped TBCCO compounds (of composition either 2212 or 2223) are thought to be determined, not only by the crystal growth defects, discussed previously, but also by a two-dimensional (2D) character of TBCCO, i.e., its high anisotropy. High anisotropy leads to a weak coupling between CuO_2 planes and consequently to a formation of weakly pinned and weakly coupled "2D-pancake" vortices.[11] Motion of these vortices is considered to be responsible for the observed high magnetic

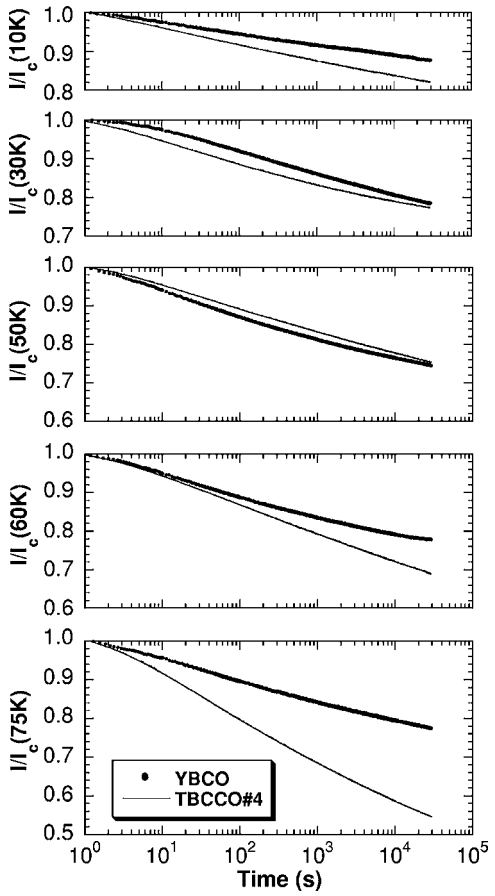

FIG. 1. Time dependence of the persistent current decaying from the critical level measured for waiting times up to 3×10^4 s in YBCO and TBCCO thin films at various temperatures between 10 and 75 K. These films have high critical current densities at 10 K of 1.5×10^7 A/cm^2 and 8.4×10^6 A/cm^2, respectively. Note similar decay rates of the current I/I_c for YBCO and TBCCO at temperatures below approximately 60 K.

relaxation rates and low values of the critical current density J_c. This is in contrast to an optimally doped YBCO, where lower relaxation rates and higher J_c are expected to result from much lower (3D-like) anisotropy.

Contrary to these ideas, TBCCO(2212) *c*-axis-oriented epitaxial thin films deposited on MgO substrates have higher than expected critical current densities around 2×10^6 A/cm^2 at 77 K, which is close to those found in epitaxial YBCO thin films at the same temperature.[12] Figure 1 presents magnetic relaxation curves measured by us at different temperatures in TBCCO and YBCO films of similar high critical current densities. In fact, these data represent decay of a transport current from its critical value in the remanent state. They show similar decay rates of the transport current J at temperatures below 60 K, suggesting that magnetic relaxation processes could be governed by similar pinning potential barriers in both TBCCO and YBCO. However, the data do not provide a definite answer to the question of what type of defect could be responsible for the observed magnetic relaxations.

Dependence of the pinning potential barrier on the current density J allows one to determine the shape of the potential well generated by a defect or a local change in the superconducting order parameter. For example, a vortex pinning potential shape described by the function $U(x)=U_p\cos(\pi x/x_p)$ (where x is the position, and U_p and x_p are the height and the width of the actual potential barrier) was considered by Beasley *et al.*[13] in studies of type II conventional superconductors. This $U(x)$ gives rise to the dependence of the effective barrier on the current density J in the presence of a Lorentz force in the following form: $U_{eff}(J)=cU_p(1-J/J_c)^{3/2}$ (where c is a constant), which approaches a linear Anderson dependence on current density[14] for J very close to J_c. In fact, a sawtooth potential shape leads to the linear $U_{eff}(J)$. Note that tilted-washboard cosine potential of the Josephson junction, of the form similar to that discussed above, yields also $U_{eff}(J)=U_p(1-J/J_c)^{3/2}$ to a good approximation.[15]

Extensive experimental studies of vortex dynamics in HTSC have allowed one to determine the empirical dependence of the vortex pinning potential on current density $U_{eff}(J)$. The most productive and unique method to find the current dependence of U_{eff} was developed by Maley *et al.*[16] This method allows one to analyze the relaxation data without any assumptions of the current and field dependence of U_{eff}. It has been applied to calculate U_{eff} over a wide range of J. Measurement of the time decay of J from its critical value J_c at a fixed temperature in YBCO, for example (over an experimentally feasible time range between 1 and 10^5 s) leads to a decrease of J by not more than 15%–20% of J_c. Maley extended the range of J by recording the decay of a magnetization from its critical value $M\propto J_c$, for various temperatures below T_c. This ensured a continuous change of J from high values at low temperatures ($J\approx J_c$) down to zero close to T_c, and permitted the calculation of $U_{eff}(J)$ over a wide range of J. Maley's procedure uses the master rate equation to calculate $U_{eff}(J,T)$ in the form

$$U_{eff}(J,T)=-kT[\ln(dM/dt)-\ln(B\omega a/\pi L)]$$
$$=-kT[\ln(dM/dt)-C], \quad (1)$$

where $C=\ln(B\omega a/\pi L)$ is the temperature-independent constant, B is the magnetic induction, ω is the microscopic attempt frequency, a is the hop distance, and L is the sample dimension. The magnetization decay rate dM/dt as a function of J can be determined from magnetic relaxation measurements taken at various temperatures between 4 K and T_c, for example. As a result, a curve of $U_{eff}(J,T)$ vs J is produced, typically not smooth, which consists of multiple segments. Each segment represents the time decay of magnetization from its critical value, measured at a specific temperature T. In order to eliminate the temperature dependence in $U_{eff}(J,T)$, this function is usually divided by a thermal factor $g(T)$ that contains the temperature dependence of superconducting parameters,[17] i.e. $U_{eff}(J,T)$ can be written as $U_{eff}(J,T)=g(T)U_{eff}(J)$, where $U_{eff}(J)$ is temperature independent. The constant C in the master equation, $U_{eff}(J,T)=-kT[\ln(dM/dt)-C]$, can be adjusted, so that $U_{eff}(J,T)/g(T)$ is a continuous function of J [i.e., all the segments of $U_{eff}(J,T)/g(T)$ form a single smooth curve].

Maley's procedure was applied very often to obtain $U_{eff}(J)$ from the magnetic relaxation data for various HTSC compounds.

Review of the available experimental data shows that so far the following three different forms of $U_{eff}(J)$ have been suggested.

(a) The power-law dependence, i.e., $U_{eff}(J) \simeq U_p[(J_c/J)^{\mu}-1]$. According to the collective pinning theory,[18] the barrier against vortex motion for $J \ll J_c$ is $U_{eff}(J) \simeq U_p(J_c/J)^{\mu}$, which gives rise to the time dependence of the current density J in the form $J(t) \simeq J_c[(kT/U_p)\ln(t/t_0)]^{-1/\mu}$. The interpolation formula that connects this power-law expression $U_{eff}(J)$ to a linear Anderson dependence on J, i.e., $U_{eff}(J)=U_p(1-J/J_c)$ for $J_c-J \ll J_c$, was suggested in the form shown previously. It corresponds to $J(t) \simeq J_c[1+(\mu kT/U_p)\ln(1+t/t_0)]^{-1/\mu}$. $U_{eff}(J) \simeq U_p[(J_c/J)^{\mu}-1]$ therefore covers a wide range of current densities[19] (including those very close to J_c) and ensures that $U_{eff}=0$ at J_c. $U_{eff}(J)$ diverges, however, as J approaches zero, thus $U_{eff}(J=0) \neq U_p$. The coefficient μ in this formula is a function of both temperature and magnetic field. It also depends on the dimensionality of the problem and on a particular regime of vortex motion. The power-law dependence was applied by experimentalists most often in an attempt to determine the effect of the driving force (i.e., the Lorentz force) on the height of the effective barrier against motion of a vortex. The values of the exponent μ over a given temperature or magnetic field range were usually determined from a $\ln[U_{eff}(J)]$ vs $\ln(J)$ graph. There are, however, some problems with this form of $U_{eff}(J)$. First of all, a very broad range of values for μ has been reported in the literature, showing a strong sample dependence of this coefficient. Very often they do not agree with those derived from models of various regimes of vortex pinning and motion.[20]

(b) The logarithmic dependence, i.e., $U_{eff}(J) \simeq U_p \ln(J_c/J)$. This empirical dependence was derived from experimental voltage-current characteristics ($\varrho-J$ characteristics) measured in YBCO thin films close to T_c.[21] Similarly to the power-law $U_{eff}(J)$, the logarithmic $U_{eff}(J)$ also diverges as $J \to 0$. The logarithmic dependence can be obtained from the power-law dependence by assuming a single-vortex pinning regime, i.e., a large exponent $1/\mu$. In this case $J(t) \simeq J_c[1+(\mu kT/U_p)\ln(1+t/t_0)]^{-1/\mu}$ could be approximated by $J(t) \simeq J_c(1+t/t_0)^{-kT/U_p}$ with a logarithmic $U_{eff}(J) \simeq U_p \ln(J_c/J)$ barrier.[22] The shape of pinning potential that produces this type of $U_{eff}(J)$ was suggested.[21] It is described by a linear function in the core of the potential well, i.e., by $U(x)=ax/x_0$ for $0 \leqslant x \leqslant x_0$ (where a and x_0 are the energy and the position scaling factors). The linear dependence is converted into the logarithmic one outside the core, i.e., $U(x)=a[\ln(x/x_0)+1]$ for $x \geqslant x_0$. There is some confusion in the literature regarding when and where the logarithmic $U_{eff}(J)$ should be applied. Very often both the logarithmic and the power-law dependence of U_{eff} on J are applied interchangeably in different temperature regions in the analysis of vortex dynamics of HTSC.

(c) The exponential dependence, i.e., $U_{eff}(J) \approx U_p \exp(-J/J_c)$. It was first introduced by Thompson *et al.*[23] after measuring long-term magnetic relaxations in YBCO crystals. They found that the time decay of magnetization is well described by an empirical double-logarithmic relation of the form $M(t)=M_0+a(T)\ln[\ln(t/t_{eff})]$, where M_0, $a(T)$, and t_{eff} are the fitting parameters. The exponential $U_{eff}(J)$ was obtained under the assumption that the deviation from a logarithmic decay is due to the dependence of U_p on J. Their experiments show that when J is close to J_c, U_{eff} is exponentially dependent on J. The exponential dependence of the form $U_{eff}(J) \propto \exp(-J/J_{co})$ was utilized by Zhu *et al.*[24] in order to explain the electrical transport and magnetic properties of epitaxial YBCO thin films studied at temperatures close to T_c. The exponential $U_{eff}(J)$ was also obtained from magnetic relaxation measurements in zone-melted YBCO and Tl-based superconductors.[25,26] The exponential $U_{eff}(J)$ approaches a final value at $J=0$. The problem is, however, that while $U_{eff}(J)$ decreases quickly with an increasing J, it does not vanish at J_c.

In spite of the initial interest in the exponential dependence of $U_{eff}(J)$ on J, this form has not been explored to the same extent as the power-law and the logarithmic dependencies. Our early investigations of vortex dynamics in YBCO thin films revealed that for current densities larger than approximately $0.4J_c$, $U_{eff}(J)$ can be expressed in the form $U_{eff}(J)=a(1-T/T^*)^{3/2}\exp(-bJ/J_{co})$, where a and b are constants.[27] T^* is the temperature above which the temperature dependence of the critical current density $J_c(T)$ deviates from a Ginzburg-Landau-like dependence of the form $J_c(T)=J_{co}(1-T/T^*)^{3/2}$ that is observed in YBCO films at temperatures below $0.4-0.6T_c$. The constant b in the exponential function $\exp(-bJ/J_{co})$ is very close to $4.7(=3\pi/2)$ for all nine YBCO films studied. It was found to be independent of thin film growth conditions, film thickness, substrates, and the magnitude of J_c and T_c.

Our purpose in this paper is to illustrate that the exponential $U_{eff}(J)$ could be used as the general dependence of the pinning potential in HTSC on current density J at high currents, i.e., for $J \gtrsim 0.4J_c$. This is based on (a) our studies of magnetic relaxations in six different TBCCO films and an analysis of the corresponding $U_{eff}(J)$; (b) the examination of $U_{eff}(J)$ obtained by two other independent research groups from magnetic relaxations measured in TBCCO and YBCO single crystals,[28,29] and (c) previous studies of magnetic relaxations in YBCO films.[27] We discussed the pinning potential shape and the associated defects that could give rise to the exponential $U_{eff}(J)$.

II. EXPERIMENTAL PROCEDURE

A. Sample characterization

The magnetic relaxation experiments were performed on six TBCCO thin films with different superconducting transition temperatures and critical current densities. Four of these films were close to the optimum doping. The remaining two were underdoped. All the films were c-axis oriented and deposited on either a $LaAlO_3$ or MgO substrate using the pulsed laser deposition followed by an annealing. TBCCO films numbered 1–3 were deposited by CTF, and those with

TABLE I. Parameters that describe TBCCO thin films No. 1–6, TBCCO crystal (Ref. 28), and an irradiated YBCO crystal (Ref. 29), which were used in the analysis of magnetic relaxations. The YBCO crystal was irradiated to have field-equivalent defect densities (matching field) B_ϕ=24 kG. Note that the values of J_c for the irradiated YBCO crystal are listed for an applied field of 5 kG.

Sample	Composition	T_c(K)	Thickness	J_c(A/cm^2) (10 K)	J_c(A/cm^2) (77 K)	Substrate	Reference
TBCCO (film) No.1	(2212)	99	500 nm	8.8×10^5	4.0×10^4	$LaAlO_3$	This work
TBCCO (film) No.2	(2212)	89	480 nm	1.2×10^6	4.0×10^5	$LaAlO_3$	This work
TBCCO (film) No.3	(2223)	101	500 nm	2.4×10^6	2.4×10^5	$LaAlO_3$	This work
TBCCO (film) No.4	(2212)	104	650 nm	8.4×10^6	1.1×10^6	MgO	This work
TBCCO (film) No.5	(2212)	103	650 nm	8.4×10^6	9.5×10^5	MgO	This work
TBCCO (film) No.6	(2212)	105	650 nm	6.8×10^6	8.7×10^5	MgO	This work
TBCCO (crystal)	(2212)	105	150 μm	3.0×10^5	—	—	Chowdhury *et al.* (Ref. 28)
YBCO (irrad. cryst.)	(123)	92	20 μm	8.0×10^6	2.0×10^5	—	Thompson *et al.* (Ref. 29)

numbers 4–6 by STI (Superconductor Technologies Inc.). The parameters that characterize these films, i.e., T_c(K), thickness, J_c(A/cm^2) at 10 and 77 K, and a substrate on which they were deposited, are listed in Table I.

B. Measurement technique

A standard technique to measure critical current is the four-probe technique that allows one to measure a resistive voltage if an applied current (generated by a constant current source) exceeds a critical current value. A disadvantage of this technique is that the magnitude of I_c is determined arbitrarily by the value of the resistive voltage ("voltage criterion") chosen by an experimentalist.

Our experimental technique was designed to avoid these types of problems. We patterned the films (which were initially square shaped) using photolithography techniques into rings, with the ring's axis pointing along the c axis of the film. The inner and outer diameters of these rings were 5.0 and 8.5 mm, respectively. A ring-shaped sample was used to generate a resistanceless (persistent) circulating current at the critical level in a film. The critical current measurement procedure using persistent-mode rings is as follows. We induce a persistent current in a ring by applying an external magnetic field B_{ext} and subsequently reducing it to zero with a rate dB_{ext}/dt. The magnetic field at the ring's center drops then to a value corresponding to the persistent current's self-field. The current is inferred from the self-field by using the Biot-Savart law. In order to produce the persistent current at the critical level, consecutively higher and higher rates of dB_{ext}/dt are applied, which result in higher and higher persistent currents. When dB_{ext}/dt exceeds a certain value (which could be called a "threshold" value), one cannot increase the persistent current anymore, and the critical level of the current is reached. This "threshold" value separates two regimes: If $dB_{ext}/dt < (dB_{ext}/dt)_{threshold}$, persistent currents of the magnitudes less than I_c are generated. For $dB_{ext}/dt > (dB_{ext}/dt)_{threshold}$, persistent currents of the magnitude equal to I_c are always produced. Since the electric field E is proportional to dB_{ext}/dt [i.e., $E \simeq (dB_e/dt)(r/2)$, where r is the ring's radius], we estimated that E=0.18 μV/cm would roughly correspond to the "threshold" value of $dB_{ext}/dt = 10^{-2}$ T/s for high J_c samples at 10 K. This "threshold" value is sample dependent and cannot be changed in our experiment. One cannot generate a critical current when dB_{ext}/dt is less than the "threshold" value. For example, applying a smaller dB_{ext}/dt that corresponds to E =0.018 μV/cm would always lead to persistent currents of magnitude less than I_c. Immediately after the external field drops to zero, the electric field is reduced approximately to the $10^{-5}-10^{-4}$ μV/cm level. These values are determined by the magnetic flux motion in a sample and temperature. The measurements are normally repeated for several higher external magnetic fields in order to ensure that the self-field and the current reached their maximum critical level. The magnitude of the persistent current is determined from its magnetic self-field, since the self-field at any point in space around the ring is directly proportional to the current according to the Biot-Savart law. The self-field of the persistent current and its time-decay due to the motion of magnetic vortices in a superconductor are monitored with an axial Hall sensor. A more detailed description of this technique was reported by us before in Ref. 27.

The time decay of the persistent current from its maximum level was recorded over waiting times between 1 and 30 000 seconds at different temperatures ranging from 10 K up to T_c.

C. Data analysis

Measurements of the time decay of the persistent current from its maximum (critical) level as a function of temperature allowed us to determine (a) the temperature dependence of the critical current density $J_c(T)$, and (b) the dependence of the effective vortex pinning potential barrier on current density $U_{eff}(J)$.

The latter was calculated using Maley's technique.[16] The outline of this technique is presented in the Introduction. We used a modified version of Maley's master equation for $U_{eff}(J,T)$, which describes relaxation of the persistent current [decay of the persistent current's self-field (local magnetic induction)] in a superconducting ring (see Ref. 27). In this case the effective barrier can be written in the following form:

$$U_{eff}[J(t),T] = -kT\ln\left(\frac{dJ(t)}{dt}\right) + kT\ln\left(\frac{J(t)\omega_0 a}{R_i}\right), \quad (2)$$

where R_i is the inner radius of the ring, ω_0 the attempt frequency, and a the hop distance. In this equation $U_{eff}[J(t),T]$ is governed mostly by the decay rate $dJ(t)/dt$. This rate can be replaced with the fractional decay rate of the current, i.e., $dJ(t)/dt/J(t)$. Then $U_{eff}[J(t),T]$ has the form

$$U_{eff}[J(t),T] = -kT\left[\ln\left(\frac{dJ(t)}{dt}/J(t)\right) - C^*\right], \quad (3)$$

where $C^* = \ln(\omega_0 a/R_i)$ is the constant that is independent of a magnetic field or a current.

Measurements of $dJ(t)/dt/J(t)$ as a function of an increasing temperature, starting at 10 K, allowed us to calculate $U_{eff}(J,T) = g(T)U_{eff}(J)$ as a function of a decreasing J. In order to obtain the pure dependence of U_{eff} on J one should separate a temperature-dependent factor $g(T)$ in $U_{eff}(J,T)$ from $U_{eff}(J)$ that depends only on the current density J. Several functional forms of $g(T)$ have been explored using heuristic arguments. Power laws $(1-T/T_c)^n$ or $(1-T/T_{irr})^n$ with $n \simeq 1.5-1.8$, and $1-(T/T_c)^2$ or $1-(T/T_{irr})^2$ (where T_{irr} is the field-dependent irreversibility line temperature), containing temperature dependence of superconducting parameters, have been often used to fit flux creep data at low and high temperatures.[24,29,30] The contribution of two forms of $g(T)$, i.e., $1-(T/T_c)^2$ and $(1-T/T_c)^{3/2}$ to scaling of $U_{eff}(J)$ at low temperatures was investigated by McHenry *et al.*[30] They found that the scaling of $U_{eff}(J)$ using $g(T) = (1-T/T_c)^{3/2}$ is better than that, which uses $g(T) = 1-(T/T_c)^2$, since the former allows for the smooth variation of $U_{eff}(J)$ with the same constant C for all magnetic fields. However, they concluded that it is more reasonable to assume a temperature dependence that flattens out at low temperatures. The problem is that many researchers assume that the superconducting properties of HTSC perovskites can be described using only a single superconducting component with $g(T) = 1-(T/T_c)^2$ or similar (see Thompson *et al.*,[29] for example), which is characterized by a flat temperature dependence at low temperatures.

Our experimental data have shown (see the figures in the Yan *et al.* paper[31]) that the superconducting properties of HTSC samples (films and crystals) are governed by two superconducting components, each with a different form of $g(T)$. Two forms of $g(T)$ are displayed directly by $I_c(T)$. $I_c(T)$ is the sum of two universal components that are sample independent. They are governed by different temperature dependence of superconducting parameters: (a) the first one with $g_1(T) \approx 1-(T/T_c)^2$, which has a temperature-independent region at low temperatures, and the $(1-T/T_c)^{3/2}$ Ginzburg-Landau (GL) tail close to T_c. This $g(T)$ is similar to that originally suggested by Tinkham.[32] (b) The second one with $g_2(T) = (1-T/T^*)^{3/2}$, which dominates at low temperatures. This form of $g(T)$ is a GL extension to low temperatures, which is expected to occur for quasi-1D superconducting filaments (or stripelike features) with a reduced order parameter.[33] The ratio of $g_1(T)$ and $g_2(T)$ in $I_c(T)$, and T^* in $g_2(T)$, are sample dependent. Temperature dependence of these two components contributes separately into scaling of $U_{eff}(J) = U_{eff}(J,T)/g(T)$. Therefore in this two-component superconducting system, one should use scaling $U_{eff}(J,T)/g_2(T)$ at high currents (low temperature) and $U_{eff}(J,T)/g_1(T)$ at low currents (high temperature) in order to determine $U_{eff}(J)$.

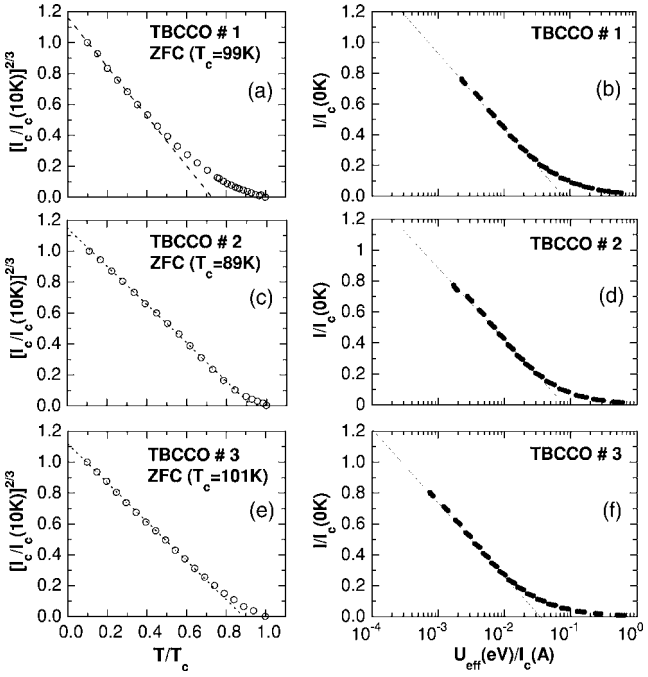

FIG. 2. Dependence of the critical current on temperature plotted as $[I_c(T)/I_c(10\text{ K})]^{2/3}$ vs T/T_c in (a), (c), and (e) on the left, compared with the dependence of U_{eff}/I_c on the current $I/I_c(0\text{ K}) = J/J_{co}$, shown in (b), (d), and (f) on the right, for low J_c TBCCO thin films No. 1–3. Note that $(U_{eff})/I_c$ approaches an exponential dependence on $I/I_c(0\text{ K}) = J/J_{co}$ for currents larger than approximately $0.3I_c(0\text{ K})$. This happens in the low-temperature regime where $I_c(T)$ reaches $I_c(T) = \text{const}(T^* - T)^{3/2}$. See the text for more details.

Our experimental procedure applied by us to obtain $U_{eff}(J)$ involved first the calculation of $U_{eff}(J,T)$ as a function of J from Eq. (3) using the magnetic relaxation data $J(t)$ that were taken over a time interval from 1 up to 30 000 seconds at different temperatures between 10 K and T_c. This was followed by plotting $U_{eff}(J,T)/g(T)$ vs J/J_{co}, where J_{co} is the critical current density at $T=0$ K. The form of $g(T)$ was determined from the temperature dependence of the critical current, as shown previously. A continuous $U_{eff}(J,T)/g(T)$ vs J/J_{co} curve was produced by adjusting the value of the constant C^*.

III. EXPERIMENTAL RESULTS

Temperature dependence of the critical current $I_c(T)$, together with the dependence of $U_{eff}(I,T)$ on the current I, are presented in Figs. 2 and 3 for TBCCO thin films No. 1–6. The segments seen in Figs. 2(b), 2(d), 2(f), 3(b), 3(d), and 3(f) represent the collection of data points obtained from the

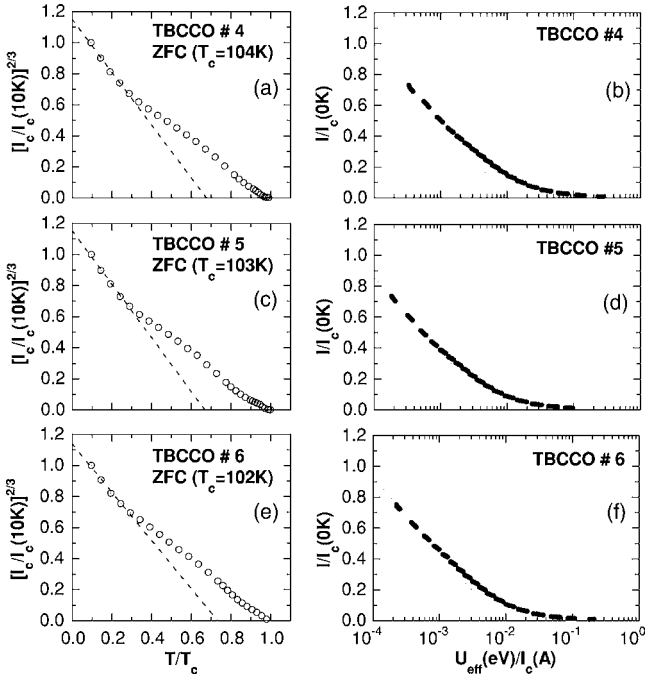

FIG. 3. Dependence of the critical current on temperature plotted as $[I_c(T)/I_c(10\ \mathrm{K})]^{2/3}$ vs T/T_c in (a), (c), and (e) on the left, compared with that of U_{eff}/I_c on the current $I/I_c(0\ \mathrm{K})$, shown in (b), (d), and (f) on the right, for high-J_c TBCCO thin films No. 4–6. Note that U_{eff}/I_c approaches an exponential dependence on $I/I_c(0\ \mathrm{K})=J/J_{co}$ for currents larger than approximately $0.4I_c(0\ \mathrm{K})$. This happens in the low-temperature regime, where $I_c(T)$ reaches $I_c(T)=\mathrm{const}\ a(T^*-T)^{3/2}$. See the text for more details.

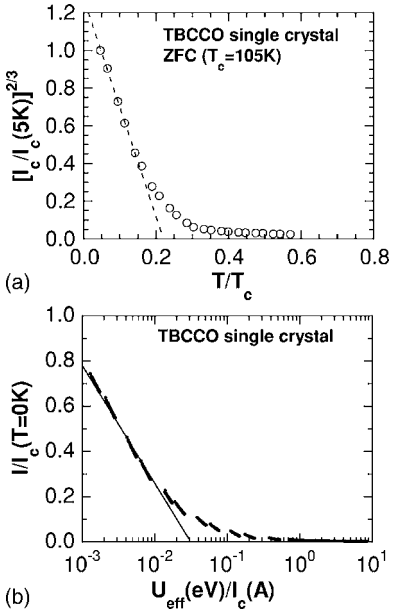

FIG. 4. Dependence of the critical current on temperature and that of the effective pinning energy barrier on the current, replotted for the TBCCO single crystal. The raw data were recorded by Chowdhury *et al.* (Ref. 28). (a) and (b) show these data replotted as $[I_c(T)/I_c(10\ \mathrm{K})]^{2/3}$ vs T/T_c, and as $I/I_c(0\ \mathrm{K})$ vs U_{eff}/I_c. Note that in (b), U_{eff}/I_c approaches an exponential dependence on $I/I_c(0\ \mathrm{K})=J/J_{co}$ for currents larger than approximately $0.3I_c(0\ \mathrm{K})$. See the text for more details.

$J(t)$ curves at temperatures between 10 K and T_c. The temperature difference between adjacent segments is 5 K. The length of each segment indicates the decay in J. Figure 2 and Fig. 3 show results for low-J_c and high-J_c TBCCO thin films, respectively. The temperature dependence of I_c at low temperatures is similar for all TBCCO samples and YBCO samples,[27] i.e., $I_c(T)=I_{co}(1-T/T^*)^{3/2}$. This could be observed if one plots $I_c(T)$ as $[I_c(T)/I_c(10\ \mathrm{K})]^{2/3}$ vs T/T_c, which yields straight lines at low temperatures. In Figs. 2(b), 2(d), 2(f), 3(b), 3(d), and 3(f), we plotted U_{eff}/I_c vs $I/I_c(0\ \mathrm{K})$ (the value of I_c at $T=0$ K was estimated by extrapolating $[I_c(T)/I_c(10\ \mathrm{K})]^{2/3}$ to a zero temperature). This dependence was plotted for different constants C^* [see Eq. (3)] until the segments seen in Figs. 2 and 3 formed a continuous curve. The best matching was achieved with $C^*=7$. One could see that for J larger than approximately $0.4J_{co}$, the dependence of U_{eff}/I_c on $I/I_c(0\ \mathrm{K})=J/J_{co}$ can be expressed by an exponential function for all TBCCO films investigated. This happens in the regime where $I_c(T)=I_{co}(1-T/T^*)^{3/2}$, i.e., where it exhibits a Ginzburg-Landau-like (GL-like) behavior. T^* could be interpreted as the temperature above which $I_c(T)$ diverges from a GL-like form. The data in Figs. 2 and 3 allowed us to write an empirical equation for $U_{eff}(J)$ in the following form:

$$U_{eff}(J) = aI_c \exp[-bI/I_c(0\ \mathrm{K})] = aI_{co}(1-T/T^*)^{3/2} \exp(-bJ/J_{co}), \quad (4)$$

where a and b are constants, and I_{co} is the critical current at $T=0$. This form of $U_{eff}(J)$ is very similar to that found earlier for YBCO(123) thin films.[27]

In order to verify that the exponential $U_{eff}(J)$ in the form shown in Eq. (4) is not affected by any experimental conditions (i.e., a local or a global measurement of magnetization), we analyzed the magnetic relaxation data measured in TBCCO(2212) and YBCO(123) crystals, which were provided to us by two independent research groups.

Magnetic relaxation studies of the TBCCO crystal were originally performed by Chowdhury *et al.*[28] They measured the time decay of a bulk remanent magnetization M_{rem} using a SQUID (superconducting quantum interference device) magnetometer. The sample was first zero-field-cooled down to a low temperature below T_c, then a magnetic field was applied along the c axis of the crystal. The measurement of magnetic relaxation commenced after the applied field was removed. $M_{rem}(t)$ was recorded over a time period from 60 s up to 3600 s at different temperatures between 5 and 60 K. $U_{eff}(J)$ was calculated using Eq. (1). We replotted the raw data for $I_c(T)$ and $U_{eff}(I,T)$ obtained by Chowdhury *et al.*[28] in Figs. 4(a) and 4(b). At high currents (low temperature), $I_c(T)=I_{co}(1-T/T^*)^{3/2}$, which is revealed by plotting $[I_c(T)/I_c(10\ \mathrm{K})]^{2/3}$ vs T/T_c in Fig. 4(a). We plotted U_{eff}/I_c in Fig. 4(b) according to the procedure applied by us earlier for TBCCO thin films. The best alignment of segments was achieved by choosing a constant $C\approx 0$ in Eq. (1). U_{eff}/I_c plotted versus $I/I_c(0\ \mathrm{K})=J/J_{co}$ implies that $U_{eff}(J)$ approaches an exponential dependence on J shown in Eq. (4) for J approximately larger than $0.3-0.4J_{co}$. This corresponds to the regime where $I_c(T)=I_{co}(1-T/T^*)^{3/2}$.

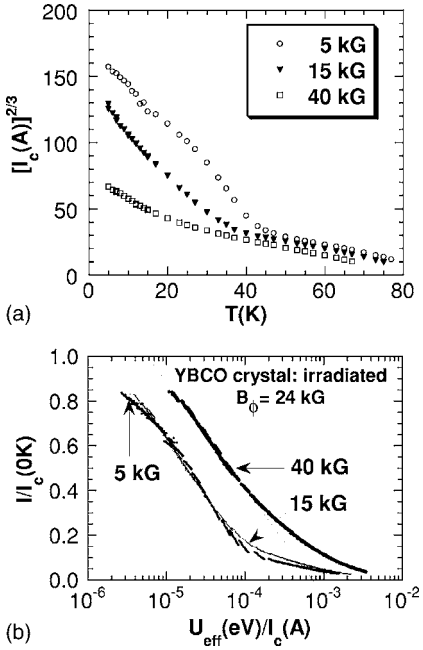

FIG. 5. Dependence of the critical current on temperature and that of the effective pinning energy barrier on the current, replotted for an irradiated YBCO single crystal in the presence of external magnetic fields of 5, 15, and 40 kG. The raw data were recorded by Thompson *et al.* (Ref. 29). (a) and (b) show these data replotted as $[I_c(T)/I_c(10\ \mathrm{K})]^{2/3}$ vs T/T_c, and as $I/I_c(0\ \mathrm{K})$ vs U_{eff}/I_c. Note that in applied fields of 15 and 40 kG, U_{eff}/I_c approaches an exponential dependence on $I/I_c(0\ \mathrm{K})=J/J_{co}$ for currents larger than approximately $0.4I_c(0\ \mathrm{K})$. See the text for more details.

Magnetic relaxation studies of an irradiated YBCO crystal (characterized by a columnar defect-matching field $B_\phi=24$ kG) were carried out by Thompson *et al.*[29] using a SQUID magnetometer in the presence of a magnetic field up to 40 kG. After zero-field-cooling down to a temperature below T_c, a fully developed critical remanent state was established in this crystal by first increasing a magnetic field (applied parallel to the columnar defects) to the maximum value of 65 kG and then reducing it to the one of target values (i.e., 5 kG, 15 kG or 40 kG). The time decay of magnetization $M(t)$ was recorded for waiting times from 60 s up to 7200 s at different temperatures between 5 and 80 K. The time-decay data were used to calculate $U_{eff}(J)$ from Eq. (1). We replotted the Thompson *et al.*[29] raw data in Figs. 5(a) and 5(b). Figure 5(a) shows the temperature dependence of the critical current $I_c(T)$ at low temperatures in the presence of an applied magnetic field, which is proportional to the factor $(1-T/T^*)^n$ with the exponent $n=1.0-1.5$. Figure 5(b) shows U_{eff}/I_c as a function of the current $I/I_c(0\ \mathrm{K})=J/J_{co}$. The best alignment of segments was obtained in this case by readjusting the constant C to 12 for applied fields of 5 and 15 kG, and to 14 for 40 kG. The dependence of U_{eff} on the current I (or the current density J) can be represented by the exponential function given by Eq. (4) for I larger than about $0.3-0.4I_{co}$ and for magnetic fields higher than 15 kG (the matching field B_ϕ is 24 kG).

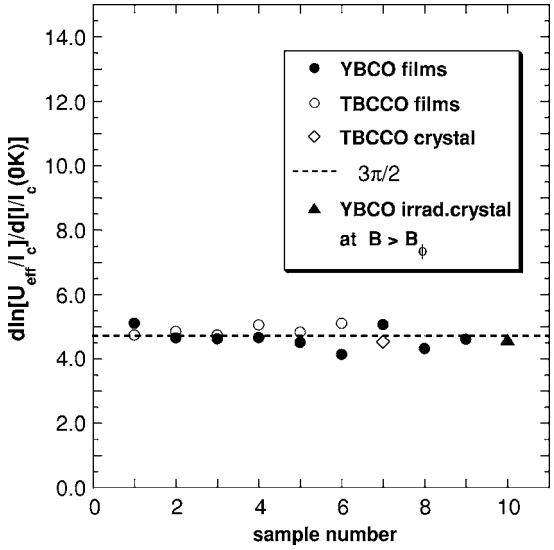

FIG. 6. The values of the constant b in Eq. (5) obtained from the dependence of U_{eff}/I_c on the current $I/I_c(0\ \mathrm{K})=J/J_{co}$ for TBCCO and YBCO films, a TBCCO single crystal, and an irradiated YBCO crystal (in the presence of a magnetic field of 40 kG that is larger than the matching field $B_\phi=24$ kG). The data for YBCO films were taken from Ref. 27. The values of b for a TBCCO crystal and an irradiated YBCO crystal are based on the magnetization data of Chowdhury *et al.* (Ref. 28) and Thompson *et al.* (Ref. 29).

IV. DISCUSSION

The experimental results for the dependence of the pinning energy barrier on the current $U_{eff}(I)$ presented in the previous section for TBCCO films, a TBCCO crystal,[28] and an irradiated YBCO crystal,[29] together with those published before for YBCO thin films[27] suggest that $U_{eff}(J)$ could be characterized by the following equation in the regime of high currents:

$$U_{eff}(J,T) = aI_{co}(1 - T/T^*)^{3/2}\exp(-bJ/J_{co}), \tag{5}$$

where a and b are constants.

$$U_{eff}(J,T=0) = aI_{co}\exp(-bJ/J_{co}) \tag{6}$$

is the pinning potential barrier that depends only on the current density J.

There are several related questions, however, that we tried to answer in this section:

(a) Is the value of the constant b in Eq. (5) the same or different for different HTSC compounds?

(b) What form of the local pinning potential $U(x)$ gives rise to the exponential $U_{eff}(J)$?

(c) What is the physical significance of the prefactor aI_{co} in Eq. (6)?

(d) What is the physical origin of b?

(e) Is b related to the spatial dependence of $U(x)$?

The calculation of the slope of the solid lines in Figs. 2(b), 2(d), 2(f), 3(b), 3(d), 3(f), 4(b), and 5(b) gives $b \simeq 4.7(=3\pi/2)$ for all samples investigated. The values of b for these samples are shown in Fig. 6. The spatial dependence of the local pinning potential $U(x)$ that gives rise to the observed exponential dependence of the pinning barrier on

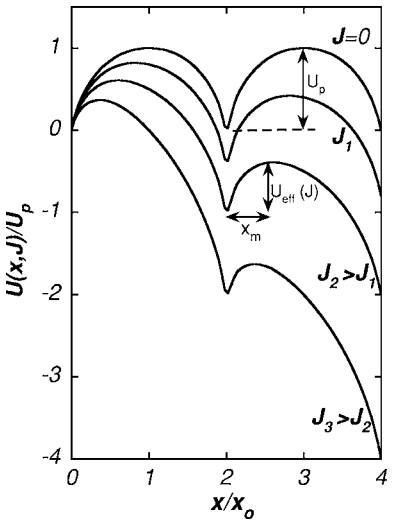

FIG. 7. Schematic representation of the spatial dependence of the periodic pinning potential $U(x)/U_p$ that gives rise to the exponential form of $U_{eff}(J)$ described by Eq. (6). The curve marked with $J=0$ is an undisturbed pinning potential in the absence of a Lorentz force. The curves labeled with the current densities J_1, J_2, and J_3 represent the pinning potential in the presence of an increasing current (an increasing Lorentz force).

current density [Eq. (5)] was suggested by Qin *et al.*[25] It is known that $U(x)$ suggested by Anderson-Kim is proportional to x for $x \leqslant x_0$, however, $U(x)$ is constant for $x \geqslant x_0$. This results in a linear dependence of U_{eff} on J. Since $U_{eff}(J)$ given by Eq. (6) is a nonlinear function, $U(x)$ should contain a nonlinear term. Qin *et al.* assumed that in this case $U(x)$ could be represented by the following function:

$$U(x) = U_p\{(x/x_0)[1 - \ln(x/x_0)]\}, \tag{7}$$

where U_p is the maximum of the pinning potential at $x=x_0$, and x_0 is the range of the pinning potential.

The spatial dependence of $U(x)$ in the absence of a driving (Lorentz) force is shown in Fig. 7 as the curve labeled with $J=0$. In the presence of the driving force due to an external current, the effective vortex pinning potential $U(x,J)$ can be written as

$$\begin{aligned} U(x,J) &= U(x) - (JBV/c)x \\ &= U_p\{(x/x_0)[1 - \ln(x/x_0)]\} - (JBV/c)x, \end{aligned} \tag{8}$$

where V is the flux volume. $(JBV/c)x$ represents a decrease in the height of the barrier due to applied forces.[13] The curves marked with J_1, J_2, and J_3 in Fig. 7 show changes in the pinning potential represented by Eq. (8) as a function of an increasing current density (an increasing Lorentz force). $U(x,J)$ has a maximum at $x=x_m$ given by the expression

$$x_m = x_0 \exp(-JBVx_0/cU_p). \tag{9}$$

The dependence of U_{eff} on J equals that of $U(x,J)$ on x_m, i.e.,

$$U_{eff}(J) = U(x_m,J) = U_p \exp(-J/\alpha), \tag{10}$$

where $\alpha=cU_p/BVx_0$. Note that the width of the pinning potential well in Fig. 7 decreases with an increasing current density J and at high enough current density it should approach ξ, the Ginzburg-Landau coherence length. At this point the pinning potential cannot be "seen" by a vortex and the critical state is reached (i.e., $J=J_c$). It is therefore the width of the pinning potential well (approximately equal to x_m at high J) that seems to determine the critical state, and not the height of the energy barrier given by Eq. (10), which does not vanish at $J=J_c$. Comparing Eq. (10) with Eq. (6) gives $U_p=aI_{co}$, and $\alpha=J_{co}/b$ or $b=J_{co}/\alpha=J_{co}BVx_0/cU_p$.

$U_p=aI_{co}$ suggests that the maximum pinning potential U_p could be related to the variation in the Josephson coupling energy $E_j=\hbar I_{co}/2e$ within the CuO_2 planes (the intraplane variation). There is growing experimental evidence of the presence of nanoscopic variations of the order parameter in the planes (nanostructures[2–4]) or in the chain layers (charge density waves[34,35]) of HTSC. It was suggested before[2] that in an optimally doped YBCO, a network of nanometer-sized cells is formed in the CuO_2 planes in order to release the lattice strain. Local oxygen redistribution could also relieve this type of strain, so the network of cells should be less likely to form locally in these cases and the superconductor becomes a filamentary (percolative) system. This suggests that the transport and magnetic properties of optimally doped HTSC samples with local disorder could be governed by two phases. Measurements performed by us on rings of optimally doped and high-J_c samples[31] revealed that $J_c(T)$ is indeed the sum of two different but universal components.

A temperature dependence of one is typical of the strongly coupled Josephson network in a nanogranular superconductor, which can carry critical current density of the order of 10^6-10^7 A/cm^2 at 10 K. It shows the Ambegaokar-Baratoff (AB) dependence at low temperatures with the Ginzburg-Landau (GL) $(1-T/T_c)^{3/2}$ tail close to T_c. According to Clem's model,[37] this type of behavior explains well $J_c(T)$ measured on strongly coupled nanogranular superconductors. The Ambegaokar-Baratoff temperature dependence of J_c was also found by Jooss *et al.*[36] in high-J_c (of the order of 10^7 A/cm^2 at 5–10 K) YBCO film grown on a vicinal substrate.

The other component is underdoped and its temperature dependence is a GL-like, i.e., $J_c(T)=J_{co}(1-T/T_c)^{3/2}$, which is observed in films and crystals at low temperatures. From the theoretical point of view, $J_c(T)=J_{co}(1-T/T_c)^{3/2}$ is expected to characterize quasi-1D superconducting filaments with a reduced order parameter.[33] In fact, this component and the AB component described above are related through the microstructure. This was discovered by performing careful annealing of YBCO films at 175 °C in argon, which causes oxygen to redistribute and come out of the sample very slowly.[38] As T_c and $J_c(T)$ drop the amount of the GL-like phase in $J_c(T)$ "seen" by the persistent current grows at the cost the AB phase. The process of change of $J_c(T)$ is reversible, i.e., $J_c(T)$ observed before annealing at 175 °C can be recovered by annealing an underdoped sample in oxygen at 500 °C.

Persistent critical current flowing in a ring allowed us to detect that the AB- and GL-like phases are intermixed. This phase separation suggests a variation of the order parameter and consequently percolative (filamentary) flow of the current in the CuO_2 planes, i.e., more precisely, the presence of a 2D array of quasi-1D superconducting filaments through which the current flows. Our data[27,31] show that the ratio of the GL-like component to the AB one in $J_c(T)$ depends on the distribution of the AB- and GL-like phases in a sample, i.e., is sample dependent.

In order to facilitate a mathematical description of vortex pinning, the properties of an array of quasi-1D filaments are modeled using Josephson junctions, since the behavior of both can be described by a mechanical analog: a particle moving in a tilted washboard potential.[39] In the case of the Josephson array, the maximum pinning potential is $U_p=fE_j$, where f is a fraction of the maximum E_j in the array.[15] In the presence of a driving force on a single vortex due to the current in the array, the factor $(JBV/c)x$ in Eq. (8) is equal to $J\phi_0(d/c)x$, where $\phi_0=hc/2e$ is the flux quantum, and d is the length of a vortex (or the array thickness).[40] Assuming that the lattice spacing of the array or the average width of a Josephson junction is a_0, the current I through the junction is Jda_0. Therefore the factor $(JBV/c)x$ can be expressed as $(JBV/c)x=J\phi_0(d/c)x=(I/da_0)(hc/2e)(d/c)x=(I/a_0)\times(h/2e)x=(I/a_0)(2\pi E_j/I_{co})x=2\pi(E_j/a_0)(I/I_{co})x$, since $h/2e=2\pi E_j/I_{co}$. $(JBV/c)x$ can be written in the final form as $2\pi(E_j/a_0)(J/J_{co})x$. Equation (8) can then be modified to handle the case of pinning in the array with $U(x,J)$ of the form

$$U(x,J)=U(x)-2\pi(E_j/a_0)(J/J_{co})x$$
$$=fE_j\{(x/x_0)[1-\ln(x/x_0)]\}-2\pi(E_j/a_0)(J/J_{co})x, \quad (11)$$

where $U(x,J)$ has a maximum at $x_m=x_0\exp[-2\pi(x_0/fa_0)\times(J/J_{co})]$. This gives the following expression for the effective pinning energy barrier $U_{eff}(J)$:

$$U_{eff}(J)=U(x_m,J)=fE_j\exp[-2\pi(x_0/fa_0)(J/J_{co})]. \quad (12)$$

Comparing this equation with Eq. (6) yields $2\pi(x_0/fa_0)\times(J/J_{co})=bJ/J_{co}$, and consequently the constant $b=2\pi(x_0/fa_0)$. According to this equation, b is governed by the magnitude of f. The experimental data shown in Fig. 7 give, in general, $b\simeq 4.7(=3\pi/2)$, therefore $x_0/fa_0=3/4$. This equation could be used to calculate the fraction $f=(4/3)\times(x_0/a_0)$ of the coupling energy E_j, which determines the maximum pinning potential $U_p=fE_j$ in Eq. (12). However, f depends also on the relationship between the pinning potential range x_0, and the cell's size a_0 in an array. One could therefore estimate f only for an assumed form of an array. For example, for a regular square array of Josephson junctions the barrier ΔE for cell-to-cell motion of the vortex could be calculated as the difference between the total energy of an array when a vortex is located between two superconducting islands (the saddle-point energy) and the energy (the minimum energy) corresponding to a vortex position between four islands[41,43] at $x_0=a_0/2$. In this case, $f=(4/3)\times(x_0/a_0)=2/3$, which means that $U_p=(2/3)E_j=0.67E_j$. For an ideal square Josephson junction array, the pinning energy was initially computed to be $\Delta E\simeq 0.2E_j$[15,42] without taking into account the magnetic self-field effects. Phillips *et al.*[43] took into account magnetic self-field effects that lead to a reduction of the effective magnetic penetration depth $\lambda_\perp$ for a 2D system[44] and to a much higher pinning energy in the Josephson array (Their calculations apply to general Josephson networks, not just square arrays). An increase of the energy barrier from about $0.2E_j$ (for $\lambda_\perp=\infty$) up to $0.5E_j$ (for $\lambda_\perp=0.7-0.8a_0$) was calculated as a function of a decreasing $\lambda_\perp$ (increasing self-field effects). This is a result of the increased localization of the vortex by the self-field effects (screening of the supercurrent of the vortex). The energy barrier obtained from our data is $0.67E_j$. Extrapolating the curve $\Delta E/E_j$ vs $\lambda_\perp$ in Fig. 7 in the Phillips *et al.* paper[43] to larger $\Delta E/E_j$ (smaller $\lambda_\perp$) gives the corresponding $\lambda_\perp\simeq 0.5a_0-0.6a_0$. Taking into account that the nanoscopic variation of the order parameter in HTSC could occur over a distance of 2–3 nm, $\lambda_\perp\simeq 1.0-1.5$ nm.

According to Tinkham,[15] a higher pinning energy in the Josephson array does not carry over directly to higher critical currents since the critical current is limited by the most weakly pinned vortex in the array, while the thermal activation measures a thermally weighted average. This appears to describe correctly the behavior of critical currents in HTSC compounds presented here, where the same exponential form of $U_{eff}(J)$ characterizes samples of various magnitudes of the critical current. Following our earlier assumption that the intrinsic pinning in HTSC could be caused by the nanostructure array, one can understand the results obtained on irradiated YBCO crystals. In an irradiated YBCO, vortex pinning is dominated by columnar defects for an applied magnetic field of the magnitude less or equal the vortex matching field $B_\phi=24$ kG, and the associated $U_{eff}(J)$ is not exponential (see Fig. 5). For applied fields higher than B_ϕ, columnar defects do not trap the magnetic flux entirely and the weaker intrinsic pinning provided by nanostructures prevails, i.e., $U_{eff}(J)$ approaches the exponential form of $U_{eff}(J)=aI_{co}\exp(-bJ/J_{co})$ with $b\simeq 3\pi/2$.

$U_{eff}(I)$ plotted on log-log and linear-log graphs supports our point of view that $U_{eff}(I)$ could be represented by the exponential dependence on the current for currents larger than $0.4I_{co}$. Figure 8 shows $\log[U_{eff}/I_c]$ plotted versus $\log(I/I_{co})$ for TBCCO films No. 1–6. For currents smaller than $0.2I_{co}$, the dependence of the pinning potential barrier on the current can be represented by the power-law dependence, i.e., $U_{eff}(I)=U_p(I/I_{co})^{-\mu}$, in agreement with the collective pinning theory[45,46] that is valid for $I\ll I_{co}$. The constant $\mu\approx 9/8$ was calculated for all six thin film samples. $U_{eff}(I)=U_p(I/I_{co})^{-9/8}$ was predicted by the collective pinning theory as the barrier against motion of vortices in the case of a 2D collective creep in layered superconductors in magnetic fields parallel to the c axis. For currents larger than $0.2I_{co}$, where the collective pinning theory is not valid, the dependence of the pinning potential barrier on the current is no longer a power-law-like (i.e., the curves show no straight-line segments). Consequently, $U_{eff}(I)$ approaches the expo-

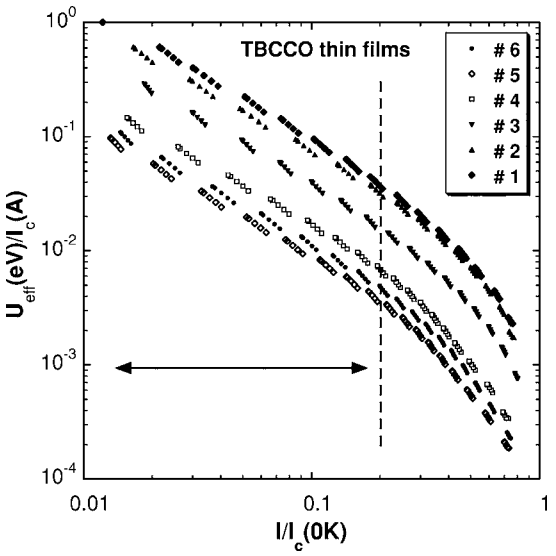

FIG. 8. Dependence of the pinning potential barrier on the current for TBCCO thin films No. 1–6, plotted as $\log[U_{eff}/I_c]$ vs $\log(I/I_{co})$, where $I_{co}=I_c(0\ \mathrm{K})$. The straight-line sections of these curves indicate that for $J \ll J_c$ (i.e., for $I \leqslant 0.2I_{co}$) the dependence of the barrier on the current $U_{eff}(I)$ can be described by the power-law $U_{eff}(I)=U_p(I/I_{co})^{-\mu}$ with $\mu \approx 9/8$, according to the 2D collective pinning theory (Refs. 45 and 46). For currents larger than $0.2I_{co}$, U_{eff}/I_c approaches the exponential dependence on $I/I_c(0\ \mathrm{K})$ (see Figs. 2 and 3).

nential dependence given by Eq. (6). Figure 9 shows the corresponding data for a TBCCO crystal and an irradiated YBCO crystal at 40 kG. These data indicate that $U_{eff}(I)$ cannot be represented by the power-law dependence for large values of the current. In the case of an irradiated YBCO, for

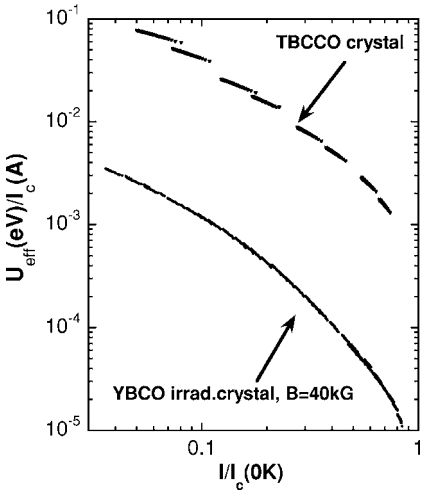

FIG. 9. Dependence of the pinning potential barrier on the current for the TBCCO crystal and an irradiated YBCO crystal at 40 kG, plotted as $\log[U_{eff}/I_c]$ vs $\log(I/I_{co})$, where $I_{co}=I_c(0\ \mathrm{K})$. The absence of straight-line sections on these curves implies that the dependence of the calculated pinning barrier on the current cannot be represented by the power-law dependence [i.e., $U_{eff}(I)=U_p(I/I_{co})^{-\mu}$, which was derived from the collective pinning theory (Ref. 18)] for any large value of the current.

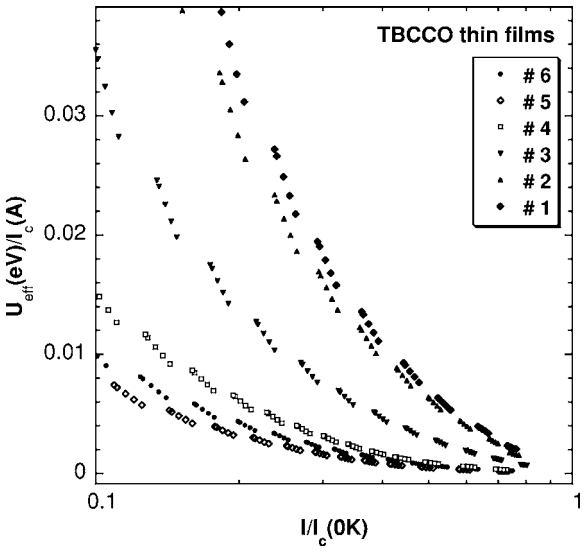

FIG. 10. Dependence of the pinning potential barrier on the current for TBCCO thin films No. 1–6, plotted as U_{eff}/I_c vs $\log(I/I_{co})$, where $I_{co}=I_c(0\ \mathrm{K})$. $U_{eff}(I)$ curves bend smoothly with an increasing current, suggesting that $U_{eff}(I)$ cannot be described by the logarithmic dependence on the current (Ref. 21) [i.e., $U_{eff}(I)=-U_p \ln(I/I_{co})$] for any value of I/I_{co}.

currents smaller than about $0.06I_{co}$, $U_{eff}(I)$ seems to approach the power-law dependence $U_{eff}(I)=U_p(I/I_{co})^{-7/9}$, which corresponds to the barrier against motion of large vortex bundles.[18] For the TBCCO crystal, on the other hand, for currents smaller than $0.1I_{co}$, the alignment of segments is worse than that for the YBCO crystal. It seems that as the current decreases $U_{eff}(I)$ approaches $U_p(I/I_{co})^{-\mu}$ with $\mu \leqslant 3/2$, which is in fact larger than that expected from the collective pinning theory for a 2D collective flux creep.

The possibility that $U_{eff}(I)$ could be represented by the logarithmic dependence on the current was tested for TBCCO films No. 1–6 by plotting the data as U_{eff}/I_c vs $\log(I/I_{co})$ in Fig. 10. The $U_{eff}(I)$ curves bend smoothly with an increasing current, suggesting that $U_{eff}(I)$ is not represented by the logarithmic barrier, i.e., $U_{eff}(I)$ is not equal to $-U_p \ln(I/I_{co})$. The same is true for an irradiated YBCO crystal. We could not perform a similar analysis for the TBCCO crystal. In this case the segments of U_{eff}/I_c vs (I/I_{co}) show very large misalignment when plotted on a linear-log graph.

V. SUMMARY AND CONCLUSIONS

We investigated the dependence of the pinning potential on current density $U_{eff}(J)$ in HTSC crystals and films, which was calculated from the magnetic (current) relaxation data. We found that for the current density $J \gtrsim 0.4J_c$, $U_{eff}(J)$ can be expressed by the empirical formula $U_{eff}(J)=aI_{co}\exp(-bJ/J_{co})$, where $b \simeq 4.7(=3\pi/2)$ is the same for all investigated samples of HTSC thin films and single crystals. This result is independent of the interplanar coupling, i.e., it is the same for both YBCO (characterized by a small anisotropy and a strong interplanar coupling) and TBCCO (characterized by a large anisotropy and a weak interplanar

coupling). We suggested that the exponential form of $U_{eff}(J)$ could be associated with the vortex pinning due to a nanoscopic variation of the order parameter within the CuO_2 planes, in agreement with the experimental evidence for the presence of nanostructures (provided, for example, by high resolution STM and TEM[2–4]) or static stripes (provided by neutron scattering data[47]). Regarding stripes, it is still believed that the properties of HTSC compounds are characterized by dynamic stripes at high oxygen doping levels, and by static stripes at low doping levels. Dynamic stripes do not act as pinning centers for magnetic vortices. The analysis of the neutron scattering data[47] for underdoped YBCO of $T_c = 50-60$ K, for example, suggested the presence of static stripes (which can pin magnetic vortices). Our earlier data[31] show that the transport properties of YBCO at low temperatures are governed by two phases: an underdoped filamentary phase of T_c around 40–60 K, and an optimally doped bulk phase. In the presence of nanostructures, stripes in the CuO_2 planes, the current could flow through a 2D network of quasi-1D superconducting filaments. A network of quasi-1D filaments behaves like a Josephson junction array, and its properties could be described using a Josephson junction description. The constant b is inversely proportional to the factor f that represents the degree of variation in the Josephson coupling energy fE_j. For a square array of Josephson junctions, for example, one should expect $b=\pi/f$ and, consequently, $f=2/3$, which gives the vortex pinning energy $U_p = 0.67E_j$. According to the model of Phillips *et al.*,[43] this energy corresponds to the pinning energy of a vortex strongly localized (due to self-field effects) in an array of Josephson junctions (or an equivalent array of quasi-1D filaments).

ACKNOWLEDGMENTS

This work was supported by the Natural Sciences and Engineering Council of Canada. We thank A. Fife for supplying us with TBCCO films. We are very much obliged to P. Chowdhury, S.-I. Lee, and J. R. Thompson for sharing with us their results obtained for TBCCO and YBCO crystals.[28,29]

*Present address: Department of Electrical and Computing Engineering, University of Calgary, Calgary, Alberta, T2N 1N4, Canada.

†Present address: King Fahd University of Petroleum and Minerals, Hail Community College, Hail, Saudi Arabia.

‡Author to whom correspondence should be addressed. Electronic address: jung@phys.ualberta.ca

[1] A. I. Larkin and Y. V. Ovchinnikov, J. Low Temp. Phys. **34**, 409 (1979).

[2] J. Etheridge, Philos. Mag. A **73**, 643 (1996).

[3] S. H. Pan, J. P. O'Neal, R. L. Badzey, C. Chamon, H. Ding, J. R. Engelbrecht, Z. Wang, H. Eisaki, S. Uchida, A. K. Gupta, K.-W. Ng, E. W. Hudson, K. M. Lang, and J. C. Davis, Nature (London) **413**, 282 (2001).

[4] K. M. Lang, V. Madhavan, J. E. Hoffman, E. W. Hudson, H. Eisaki, S. Uchida, and J. C. Davis, Nature (London) **415**, 412 (2002).

[5] C. Gerber, D. Anselmetti, J. G. Bednorz, J. Mannhart, and D. G. Schlom, Nature (London) **350**, 279 (1991).

[6] M. Hawley, I. D. Raistrick, J. G. Beery, and R. J. Houlton, Science **251**, 1587 (1991).

[7] D. H. Lowndes, D. K. Christen, C. E. Klabunde, Z. L. Wang, D. M. Kroeger, J. D. Budai, S. Zhu, and D. P. Norton, Phys. Rev. Lett. **74**, 2355 (1995).

[8] J. H. Durrell, S. H. Mennema, Ch. Jooss, G. Gibson, Z. H. Barber, H. W. Zandbergen, and J. E. Evetts, J. Appl. Phys. **93**, 9869 (2003).

[9] X. L. Wang, H. K. Liu, and S. X. Dou, Int. J. Mod. Phys. B **16**, 9 (2002).

[10] W. K. Kwok, U. Welp, G. W. Crabtree, K. G. Vandervoort, R. Hulscher, and J. Z. Liu, Phys. Rev. Lett. **64**, 966 (1990); W. K. Kwok, U. Welp, V. M. Vinokur, S. Fleshler, J. Downey, and G. W. Crabtree, *ibid.* **67**, 390 (1991).

[11] J. R. Clem, Phys. Rev. B **43**, 7837 (1991).

[12] B. A. Willemsen, K. E. Kihlstrom, T. Dahm, D. J. Scalapino, B. Gowe, D. A. Bonn, and W. N. Hardy, Phys. Rev. B **58**, 6650 (1998).

[13] M. R. Beasley, R. Labusch, and W. W. Webb, Phys. Rev. **181**, 682 (1969).

[14] P. W. Anderson, Phys. Rev. Lett. **9**, 309 (1962).

[15] M. Tinkham, *Introduction to Superconductivity* (McGraw-Hill, New York, 1996).

[16] M. P. Maley, J. O. Willis, H. Lessure, and M. E. McHenry, Phys. Rev. B **42**, R2639 (1990).

[17] P. J. Kung, M. P. Maley, M. E. McHenry, J. O. Willis, J. Y. Coulter, M. Murakami, and S. Tanaka, Phys. Rev. B **46**, 6427 (1992); P. J. Kung, M. P. Maley, M. E. McHenry, J. O. Willis, M. Murakami, and S. Tanaka, *ibid.* **48**, 13922 (1993).

[18] M. V. Feigelman, V. B. Geshkenbein, A. I. Larkin, and V. M. Vinokur, Phys. Rev. Lett. **63**, 2303 (1989).

[19] M. V. Feigelman, V. B. Geshkenbein, and V. M. Vinokur, Phys. Rev. B **43**, 6263 (1991).

[20] G. Blatter, M. V. Feigel'man, V. B. Geshkenbein, A. I. Larkin, and V. M. Vinokur, Rev. Mod. Phys. **66**, 1125 (1994), and references therein; Y. Yeshurun, A. P. Malozemoff, and A. Shaulov, *ibid.* **68**, 911 (1996).

[21] E. Zeldov, N. M. Amer, G. Koren, A. Gupta, M. W. McElfresh, and R. J. Gambino, Appl. Phys. Lett. **56**, 680 (1990).

[22] M. Nideröst, A. Suter, P. Visani, A. C. Mota, and G. Blatter, Phys. Rev. B **53**, 9286 (1996).

[23] J. R. Thompson, Y. R. Sun, and F. Holtzberg, Phys. Rev. B **44**, R458 (1991).

[24] S. Zhu, D. K. Christen, C. E. Klabunde, J. R. Thompson, E. C. Jones, R. Feenstra, D. H. Lowndes, and D. P. Norton, Phys. Rev. B **46**, 5576 (1992).

[25] M. J. Qin, X. Jin, H. L. Ji, Z. X. Shi, X. X. Yao, Z. G. Fan, and Y. Q. Shan, J. Appl. Phys. **77**, 2618 (1995).

[26] Z. X. Shi, H. L. Ji, X. Jin, X. X. Yao, X. S. Rong, Y. M. Li, H. T. Peng, X. R. Long, and C. R. Peng, Physica C **231**, 284 (1994).

[27] H. Darhmaoui and J. Jung, Phys. Rev. B **57**, 8009 (1998).

[28] P. Chowdhury, H.-J. Kim, I.-S. Jo, and S.-I. Lee, Phys. Rev. B **66**, 184509 (2002).
[29] J. R. Thompson, L. Krusin-Elbaum, L. Civale, G. Blatter, and C. Feild, Phys. Rev. Lett. **78**, 3181 (1997).
[30] M. E. McHenry, S. Simizu, H. Lessure, M. P. Maley, J. Y. Coulter, I. Tanaka, and H. Kojima, Phys. Rev. B **44**, 7614 (1991).
[31] H. Yan, J. Jung, H. Darhmaoui, Z. F. Ren, J. H. Wang, and W.-K. Kwok, Phys. Rev. B **61**, 11711 (2000).
[32] M. Tinkham, Phys. Rev. Lett. **61**, 1658 (1988).
[33] V. Z. Kresin LBNL, private communication.
[34] D. J. Derro, E. W. Hudson, K. M. Lang, S. H. Pan, J. C. Davis, J. T. Markert, and A. L. de Lozanne, Phys. Rev. Lett. **88**, 097002 (2002).
[35] H. L. Edwards, A. L. Barr, J. T. Markert, and A. L. de Lozanne, Phys. Rev. Lett. **73**, 1154 (1994).
[36] Ch. Jooss, R. Warthmann, H. Kronmuller, T. Haage, H.-U. Habermeier, and J. Zegenhagen, Phys. Rev. Lett. **82**, 632 (1999); Ch. Jooss, R. Warthmann, and H. Kronmuller, Phys. Rev. B **61**, 12433 (2000).
[37] J. R. Clem, B. Bumble, S. I. Raider, W. J. Gallagher, and Y. C. Shih, Phys. Rev. B **35**, 6637 (1987).
[38] J. Jung, K. H. Chow, and A. Welsh, to be published.
[39] N. Giordano and E. R. Schuler, Phys. Rev. Lett. **63**, 2417 (1989).
[40] E. Simanek, *Inhomogeneous Superconductors* (Oxford University Press, New York, 1994).
[41] M. S. Rzchowski, S. P. Benz, M. Tinkham, and C. J. Lobb, Phys. Rev. B **42**, 2041 (1990).
[42] C. J. Lobb, D. W. Abraham, and M. Tinkham, Phys. Rev. B **27**, 150 (1983).
[43] J. R. Phillips, H. S. J. van der Zant, J. White, and T. P. Orlando, Phys. Rev. B **47**, 5219 (1993).
[44] T. P. Orlando, J. E. Mooij, and H. S. J. van der Zant, Phys. Rev. B **41**, 10218 (1990).
[45] M. V. Feigelman, V. B. Geshkenbein, and A. I. Larkin, Physica C **167**, 177 (1990).
[46] V. M. Vinokur, P. H. Kes, and A. E. Koshelev, Physica C **168**, 29 (1990).
[47] T. Egami ORNL, private communication.